ACS Catalysis

Research Article

pubs.acs.org/acscatalysis

Nickel-Exchanged Zincosilicate Catalysts for the Oligomerization of Propylene

Mark A. Deimund, Jay Labinger, and Mark E. Davis*

Division of Chemistry & Chemical Engineering, California Institute of Technology, Pasadena, California 91125, United States

Supporting Information

ABSTRACT: Two nickel-containing zincosilicates (Ni-CIT-6 and Ni−Zn-MCM-41) and two nickel-containing aluminosilicates (Ni-HiAl-BEA and Ni-USY) are synthesized and used as catalysts to oligomerize propylene into C_{3n} (C_6 and C_9) products. Both Ni-CIT-6 and Ni-HiAl-BEA have the *BEA topology and are investigated to assess the effects of framework zinc versus aluminum because the former gives two framework charges per atom, whereas the latter, only one. Ni-CIT-6 and Ni−Zn-MCM-41 enable the comparison of a microporous to a mesoporous zincosilicate. Ni^{2+} ion-exchanged into zeolite Y has been previously reported to oligomerize propylene and is used here for comparison. Reaction data are obtained at 180 and 250 °C, atmospheric pressure, and WHSV = 1.0 h^{-1} in a feed stream of 85 mol % propylene (in inert). At these conditions, all catalysts are capable of oligomerizing propylene with steady-state conversions ranging from 3 to 16%. With the exception of Ni-HiAl-BEA, all catalysts have higher propylene conversions at 250 °C than at 180 °C. Both *BEA materials exhibit similar propylene conversions at each temperature, but Ni-HiAl-BEA is not as selective to C_{3n} products as Ni-CIT-6. Zincosilicates demonstrate higher average selectivities to C_{3n} products than the aluminosilicates at both reaction temperatures tested. Hexene products other than those expected by simple oligomerization are present, likely formed by double-bond isomerization catalyzed at acid sites. Additionally, both of the aluminosilicate materials catalyzed cracking reactions, forming non-C_{3n} products. The reduced acidity of the zincosilicates relative to the aluminosilicates likely accounts for higher C_{3n} product selectivity of the zincosilicates. Zincosilicates also exhibited higher linear-to-branched hexene isomer ratios (typically 1.0−1.5) when compared with the aluminosilicates, which had ratios on the order of 0.3. The mesoporous zincosilicate shows the best reaction behavior (including C_{3n} product selectivity: ∼99% at both temperatures for Ni−Zn-MCM-41) of the catalytic materials tested here.

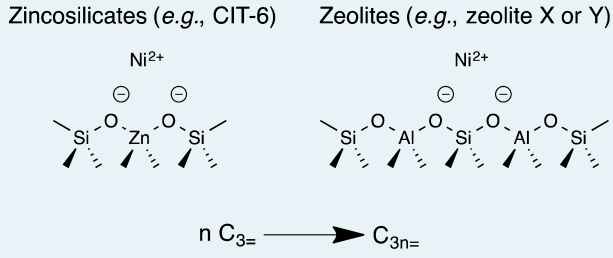

KEYWORDS: *propylene, oligomerization, nickel, zincosilicate, *BEA*

1. INTRODUCTION

Nickel-containing aluminosilicate catalysts are capable of oligomerizing light olefins (C_2−C_4) to higher molecular weight liquid hydrocarbons for blending into gasoline and distillate transportation fuel streams.[1,2] The exchange of Ni^{2+} cations into zeolites that have framework topologies such as FAU and MFI have been shown to give catalysts that can oligomerize these light olefins to liquid olefins (C_{6+}) at reaction temperatures of 25−350 °C and at pressures from slightly above atmospheric to over 35 bar.[3−8] Other aluminosilicates, such as amorphous silica−alumina combined with nickel oxide[9−11] and nickel-exchanged mesoporous materials,[12−14] are also able to perform these types of oligomerization reactions.

Although aluminosilicate materials are generally effective as oligomerization catalysts, they do exhibit some drawbacks. Because Ni^{2+} is a divalent cation, two nearby framework aluminum atoms are required to counterbalance the positive charge.[15] High aluminum content in materials such as zeolites X or Y (Si/Al molar ratio ≈ 1−3) provide an increased probability of paired aluminum sites to occur in the zeolite frameworks and thus allow for higher Ni^{2+} exchanges, but nonexchanged aluminum can yield additional Brønsted acid sites. The strong Brønsted acidity can catalyze oligomerization, but may also give undesired side reactions (such as cracking), thereby producing a wide variety of products in addition to the desired oligomers.[1] It has been shown that the Ni^{2+} ion sites alone are sufficient to perform light olefin oligomerization;[16] thus, Brønsted sites are unnecessary in the presence of the Ni^{2+} cations.

In zincosilicates, framework Zn^{2+} atoms create two anionic charges per zinc heteroatom that can accommodate the Ni^{2+} ion in a 1:1 exchange ratio, leaving no unpaired charge centers (Scheme 1). Furthermore, unexchanged zinc-based charge centers exhibit significantly reduced acidity relative to the aluminum sites.[17] The absence of strong Brønsted acidity may provide greater selectivity to the desired oligomerization products.

Here, we explore the use of zincosilicate-based catalysts for the oligomerization of light olefins. CIT-6, a zincosilicate

Received: September 2, 2014
Revised: October 14, 2014
Published: October 14, 2014

   dx.doi.org/10.1021/cs501313z | ACS Catal. 2014, 4, 4189−4195

Scheme 1. Comparison of Ni^{2+}-Exchanged Zeolites with Ni^{2+}-Exchanged Zincosilicate Molecular Sieves

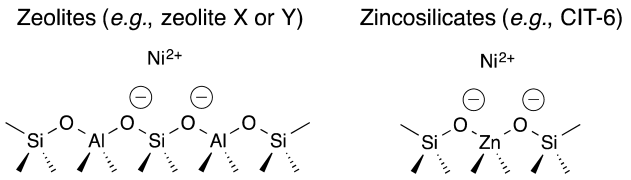

molecular sieve with *BEA topology,[18−20] is exchanged with Ni^{2+} and tested as a catalyst for converting propylene into higher olefins (C_6 and C_9 products). Additionally, we investigate high-aluminum zeolite beta (HiAl-BEA),[21−23] Zn-MCM-41,[24−26] and ultrastable zeolite Y (USY) to study the effects of (i) Al versus the Zn heteroatom in the *BEA topology and (ii) the nature of the zincosilicate solid (microporous vs mesoporous), as well as comparison with a previously studied catalyst (USY), respectively. We attempted to keep the number of Ni^{2+} exchange sites and Ni^{2+} loadings comparable among all solids (hence, the use of HiAl-BEA and USY). Similar Si/Zn and Si/(2Al) ratios are maintained, as well as Ni/Zn and Ni/(2Al) ratios, to allow for meaningful comparisons.

2. EXPERIMENTAL SECTION

2.1. Synthesis of Porous Materials. All materials (with the exception of USY) were synthesized following known recipes.[19,21,24] The zeolite USY was obtained from Zeolyst (Zeolyst CBV-712, SiO_2/Al_2O_3 = 12, NH_4^+ form).

CIT-6 was synthesized according to the method of Takewaki et al.[19] A synthesis gel of composition $1SiO_2/0.03Zn(OAc)_2/0.65TEAOH/0.05LiOH/30H_2O$ was prepared with Ludox AS-40 as the silica source, zinc acetate dihydrate (Aldrich), tetraethylammonium hydroxide (Aldrich, 35 wt % in water), and lithium hydroxide monohydrate powder (Aldrich). The gel was charged into a Teflon-lined, stainless steel autoclave and heated statically at 140 °C for 7.5 days under autogenous pressure. The crystalline white solid in the bottom of the Teflon liner was recovered by centrifugation, extensively washed with water and acetone, and dried at 100 °C overnight.

The mesoporous zincosilicate Zn-MCM-41 was synthesized in a manner similar to that described by Takewaki et al.[24] A synthesis gel of composition $1SiO_2/0.024Zn(OAc)_2/0.5NaOH/0.61CTAB/60H_2O$ was prepared with Ludox AS-40 as the silica source, zinc acetate dihydrate (Aldrich), NaOH pellets (Aldrich), and cetyltrimethylammonium bromide powder (Aldrich). The gel was charged into a Teflon-lined, stainless steel autoclave and heated statically at 110 °C for 5 days under autogenous pressure. The white solid in the bottom of the Teflon liner was recovered by centrifugation, extensively washed with water and acetone, and dried at room temperature overnight.

High-aluminum zeolite beta (HiAl-BEA) was synthesized according to a seeded procedure similar to that described by Majano et al.[21] A synthesis gel of composition $1SiO_2/0.025Al_2O_3/0.325Na_2O/25H_2O$ was prepared with Ludox AS-40 as the silica source, sodium aluminate (Alfa Aesar) as the alumina source, and a 50 wt % NaOH solution. The gel was seeded with commercial zeolite beta from Tosoh (Tosoh HSZ-930NHA, SiO_2/Al_2O_3 = 27, NH_4^+ form). The gel was homogenized and charged into a Teflon-lined stainless steel autoclave. The autoclave was heated statically at 110 °C for 6 days. The procedure for collection of the zeolite material was similar to that described for CIT-6.

2.2. Ni^{2+} Exchange and Zn Heteroatom Protection. Ni^{2+} ion exchange was performed at 75 °C (25 °C for Zn-MCM-41) for 5 h using a 0.01 M solution of $Ni(NO_3)_2$ (Sigma-Aldrich, hexahydrate) that had been pH-adjusted to 7.0 using 0.01 M NaOH solution. For each exchange, 250 mg of material was added to 25 mL of solution. The materials were then separated from the $Ni(NO_3)_2$ solution via centrifugation, washed with distilled water, and dried. After the Ni^{2+} exchange, each material exhibited a pale green color.

Calcination or acid extraction is required to remove the tetraethylammonium (TEA^+) cation from CIT-6. Some of the zinc heteroatoms can also be removed from the CIT-6 framework via this process to form ZnO particles. Thus, a means of protecting the zinc heteroatom while still allowing for removal of the organic template used in synthesis (consequently activating the catalyst) is necessary. It was determined that direct exchange of a divalent cation (Ni^{2+} used here for catalysis purposes, although Mg^{2+} or Ca^{2+} work, as well) onto the as-made material (still containing the TEA^+ cation) in a pH-neutral exchange solution, followed by calcination, could protect the framework zinc while allowing removal of the TEA^+ cation. In cases that Mg^{2+} or Ca^{2+} ions were initially exchanged (using a 1 M $MgCl_2$ or 1 M $CaCl_2$ solution, pH-adjusted to 7.0 with dilute NaOH, for 5 h at 75 °C), calcination and subsequent exchange with the Ni^{2+} cation using the procedure described above was possible. CIT-6 samples that underwent calcination without the initial exchange of Mg^{2+} or Ca^{2+} did not give good exchange of Ni^{2+} into the CIT-6 material, presumably as a result of removal of the zinc heteroatom from the framework during calcination.

Although the as-made material can have the Ni^{2+} cation directly exchanged onto it as described previously (provided the pH of the exchange solution is adjusted to 7.0) and activated via calcination, the protection via divalent cations does provide another means to protect the divalent zinc exchange site in situations where organic removal is desired but Ni^{2+} exchange is not needed.

2.3. Characterizations. The as-made materials were characterized by powder X-ray diffraction (XRD) on a Rigaku Miniflex II diffractometer with Cu Kα radiation (λ = 1.541 84 Å) to determine structure type and give an estimate of purity. In each diffraction pattern for CIT-6, HiAl-BEA, or USY, 2θ angles from 4° to 40° were acquired with a sampling window of 0.010° and a scan speed of 0.100°/min, while the X-ray source was at 30 kV and 15 mA. For Zn-MCM-41, 2θ angles from 1.5° to 40° were acquired, again with a sampling window of 0.010° and a scan speed of 0.100°/min, while the X-ray source was at 30 kV and 15 mA.

Scanning electron microscopy/energy dispersive spectroscopy (SEM/EDS) analyses were conducted on a JEOL JSM-6700F instrument equipped with an Oxford INCA Energy 300 X-ray energy dispersive spectrometer. The SEM/EDS was used to determine the morphology as well as the Si/Zn and Ni/Zn (or Si/Al and Ni/Al) of the materials.

Solid-state NMR spectroscopy was performed on a Bruker AM 300 spectrometer equipped with high power amplifiers for solids. Samples were spun at the magic angle (MAS) in 4 mm ZrO_2 rotors. ^{27}Al MAS NMR (78.2 MHz) spectra were obtained at a spinning rate of 12 kHz and referenced to a 1 M aqueous aluminum nitrate solution (0 ppm).

dx.doi.org/10.1021/cs501313z | ACS Catal. 2014, 4, 4189−4195

To quantify the number and strength of the Brønsted acid sites present in each catalyst, NH_3 temperature-programmed desorption (TPD) was performed on each nickel-exchanged, calcined material. The materials were pelletized, crushed, and sieved. Particles between 0.6 mm and 0.18 mm were supported between quartz wool beds in a continuous flow quartz-tube reactor (part of an Altamira AMI-200 reactor system). Bed temperature was monitored via a thermocouple inserted directly into the catalyst bed, and desorbing products were monitored via a Dymaxion mass spectrometer with m/z scanning capability.

Once loaded, samples were heated to 150 °C for 1 h at 10 °C/min, followed by heating to 600 °C for 1 h at 10 °C/min in flowing helium (50 sccm) to remove any adsorbed species. Samples were then cooled to 160 °C, and NH_3 was dosed onto each sample at a flow rate of 5 sccm in 50 sccm helium until no further NH_3 uptake was observed via the mass spectrometer (typically <5 min). After a 8 h purge in flowing helium (50 sccm) to remove any physisorbed NH_3, the sample was heated to 600 °C at rate of 2 °C/min in 20 sccm helium while the mass spectrometer monitored desorbing products, namely, m/z = 17 fragments corresponding to NH_3. The sample was held at 600 °C for 2 h to ensure all species had fully desorbed.

2.4. Reaction Testing. Prior to reaction testing, all materials were calcined in medical grade air. The materials were heated to 150 °C at 1 °C/min, held for 3 h at 150 °C, then heated further to 580 °C at 1 °C/min and held for 12 h, all under flowing air.

The calcined materials were pelletized, crushed, and sieved. Particles between 0.6 mm and 0.18 mm were supported between glass wool beds in an Autoclave Engineers BTRS, Jr. 316 SS continuous flow, tubular reactor.

For reaction testing, a mixture of propylene and an inert gas (composition 85 mol % propylene, balance He/Ar) was supplied to the 3/8″ ID 316 SS tubular reactor, with total flow such that a weight hourly space velocity (WHSV) of 1.0 h^{-1} was attained.

Each catalyst was tested at 180 and 250 °C after the initial calcination, as well as after a second calcination in flowing air to determine regeneration potential. In a typical run, 200 mg of dry catalyst was loaded. Reactor effluent gases were analyzed using an on-stream GC/FID/TCD Agilent GC 7890A with Plot-Q capillary columns installed. Conversions and selectivities were computed on a carbon mole basis.

3. RESULTS AND DISCUSSION

3.1. Characterization of Materials Used as Catalysts. The powder XRD patterns of the porous solids used here, after nickel exchange and calcination, are shown in Figure 1. Additional powder XRD data (for each material as synthesized, after nickel exchange, and after calcination) are shown in Figures S1−S5 of the Supporting Information (SI).

A summary of the elemental compositions (by EDS) of the solids used for reaction testing is shown in Table 1. The Si/Zn for CIT-6 (and thus, the number of sites available for Ni^{2+} exchange) is similar to the Si/(2Al) ratios in HiAl-BEA and USY because these zeolites required paired aluminum sites for the Ni^{2+} exchange. However, the Zn-MCM-41 could be reliably synthesized only at a Si/Zn ratio approximately twice that of these materials. Nonetheless, we were able to maintain a comparable number of Ni^{2+} exchange sites.

Micropore volumes for the microporous materials were determined by Ar adsorption, and volumes are consistent with

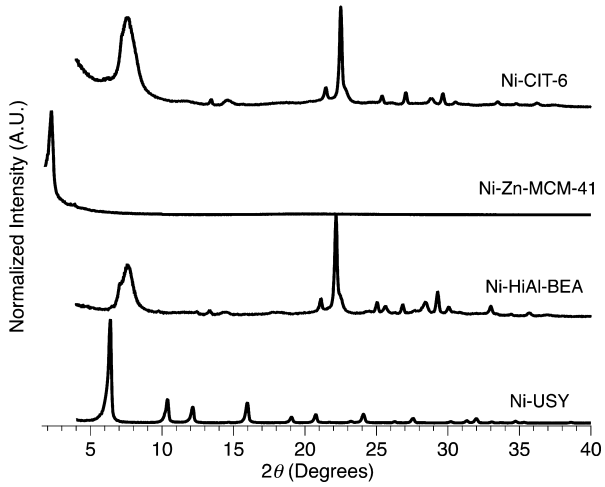

Figure 1. Powder XRD patterns of nickel-exchanged, calcined materials: Ni-CIT-6, Ni−Zn-MCM-41, Ni-HiAl-BEA, and Ni-USY.

Table 1. Elemental Compositions for Materials

material	Si/Zn	Ni/Zn
Ni-CIT-6	10.8	0.55
Ni−Zn-MCM-41	22.7	0.59
	Si/Al	Ni/Al
Ni-HiAl-BEA	4.2	0.39
Ni-USY	5.8	0.33

previously reported syntheses (Table S1 and Figures S7−S10 of the SI). ^{27}Al MAS NMR spectra were obtained for each aluminosilicate solid, and the results show only tetrahedral aluminum (Figure S6 of the SI). Ammonia TPD also show consistently fewer Brønsted acid sites in the zincosilicates as compared with the aluminosilicates (Figure S11 and Table S2 of SI).

3.2. Reaction Testing. Figure 2 illustrates typical reaction data for each of the four different catalysts tested at 180 °C. Each material, with the exception of Ni−Zn-MCM-41, exhibits decreased propylene conversion with increasing time on-stream (TOS) as the catalyst deactivates. The main C_6 products observed in all cases are 2-hexene, 2-methyl-2-pentene, and 4-methyl-2-pentene. One of those, 2-methyl-2-pentene, is likely formed via double-bond migration of the expected primary products (2-methyl-1-pentene and 4-methyl-2-pentene) at Brønsted acid sites resulting from unexchanged zinc or aluminum heteroatoms. The zincosilicates exhibited only this double-bond isomerization, whereas the aluminosilicates also catalyzed cracking reactions to form non-C_{3n} products, likely due to the relative acidic strength of the framework zinc and aluminum heteroatoms.[17] As time on-stream increases, these isomerization sites in each material deactivate, and more primary products are observed in the hexene product mixture. Selectivity to C_9 products (primarily olefins) increases with increasing TOS, and typically stabilizes by ∼100 min on-stream. Full conversion and selectivity data for each of these materials at both 180 and 250 °C are shown in Figures S12−S29 of the SI. Reaction data for the materials exchanged with Mg^{2+} or Ca^{2+} before calcination and subsequent exchange with Ni^{2+} are shown in Figure S30 of the SI.

For each material, postreaction powder XRD patterns show no loss of structure (Figure S31 of the SI). Additionally, carbon balances are typically over 95% for the duration of each reaction

dx.doi.org/10.1021/cs501313z | ACS Catal. 2014, 4, 4189−4195

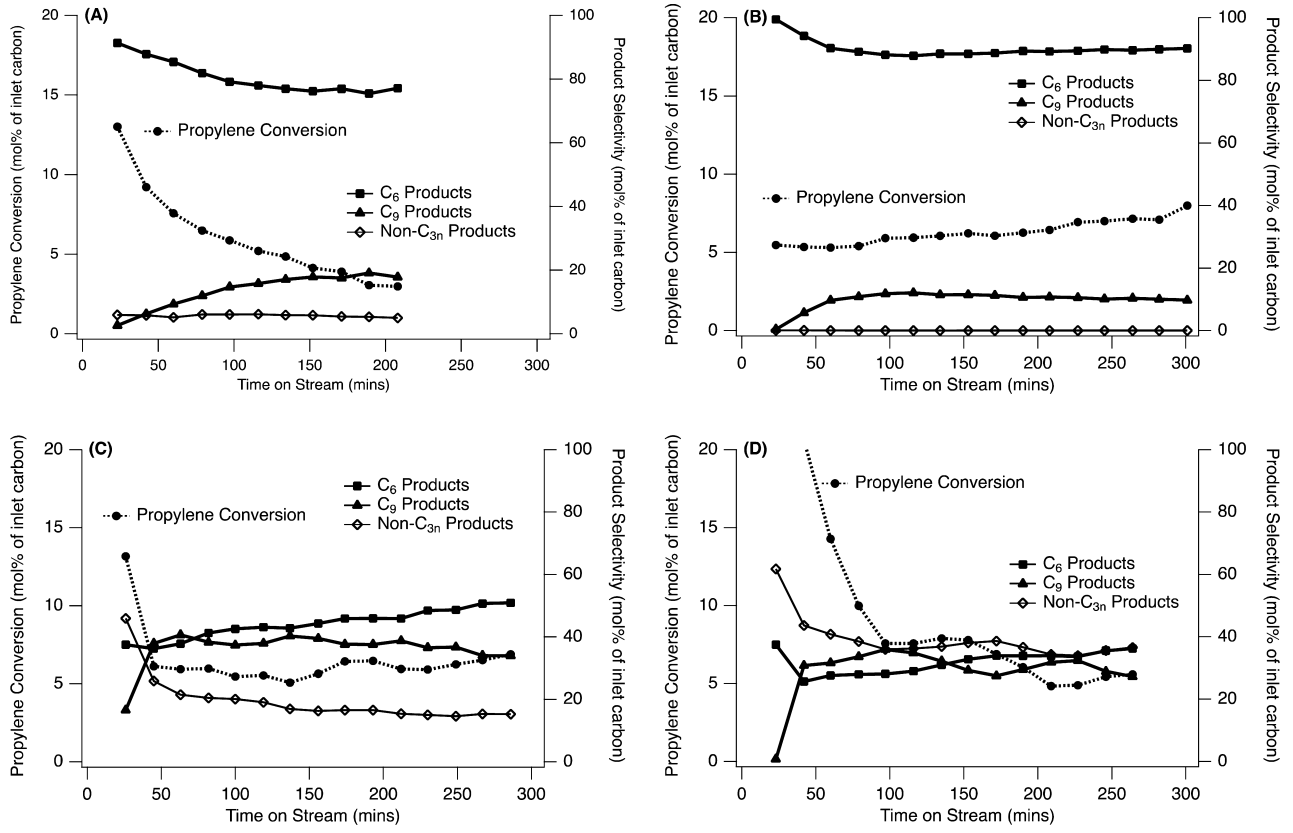

Figure 2. Representative time-on-stream profiles of conversion, C_6 and C_9 selectivity for Ni-CIT-6 (A), Ni−Zn-MCM-41 (B), Ni-HiAl BEA (C), and Ni-USY (D) at 180 °C. Lines connect data points to guide the eye.

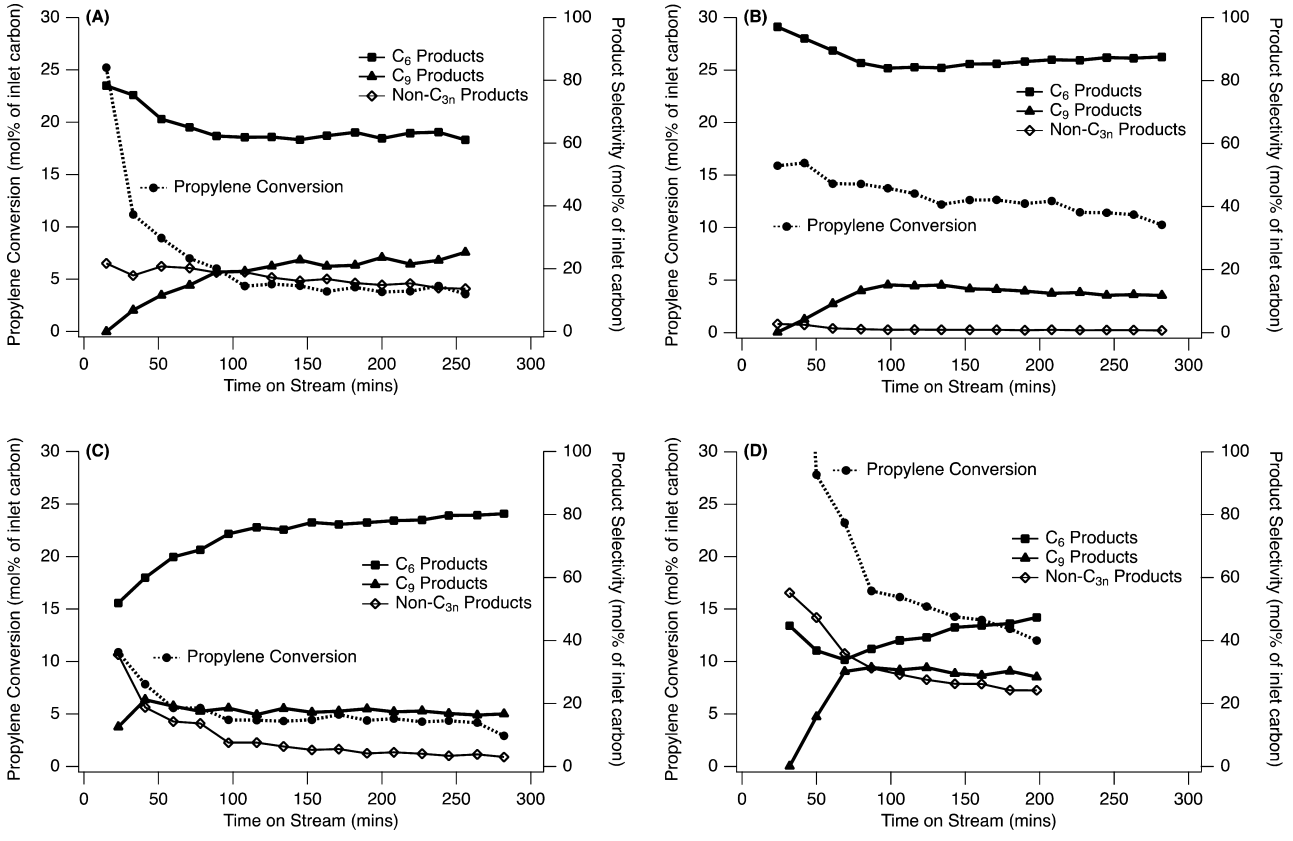

Figure 3. Representative time-on-stream profiles of conversion and C_6 and C_9 selectivity for Ni-CIT-6 (A), Ni−Zn-MCM-41 (B), Ni-HiAl-BEA (C), and Ni-USY (D) at 250 °C. Lines connect data points to guide the eye.

dx.doi.org/10.1021/cs501313z | ACS Catal. 2014, 4, 4189−4195

run, with the exception of the initial sample for the run, where propylene is likely forming coke on the sample. Postreaction thermogravimetric analysis experiments on each spent catalyst reveal mass losses above 150 °C of ∼4−15%, with less mass loss observed for the zincosilicates relative to the aluminosilicates (see Figures S32−S37 of the SI). Regeneration by calcination in flowing medical grade air recovered nearly all of the catalytic activity observed initially for each material.

Both materials with the *BEA framework (Ni-CIT-6 and Ni-HiAl-BEA) exhibit similar TOS behavior with respect to propylene conversion, but the product distribution for Ni-HiAl-BEA is not as selective to C_{3n} products as Ni-CIT-6; C_7−C_9 saturated and unsaturated products are observed in amounts comparable to that of the C_6 products. Selectivity to C_4 and C_5 saturated and unsaturated products is low (<10% total); primarily oligomerization and subsequent cracking products are observed.

The strong Brønsted acid sites in Ni-HiAl-BEA appear to catalyze cracking and isomerization, resulting in the observed C_7 and C_8 products. This suggests that the nickel ions present in the *BEA structure are similarly active for the production of simple oligomerization products with either heteroatom present (zinc or aluminum), whereas residual Brønsted acid sites in the framework are likely responsible for the observed differences in product selectivity resulting from double-bond isomerization or cracking (or both) of primary C_{3n} products.

The two zincosilicates (Ni-CIT-6 and Ni−Zn-MCM-41) exhibit by far the highest selectivities to C_{3n} oligomerization products, and Ni−Zn-MCM-41 has the most stable propylene conversion with increasing TOS. This stability observed for the Ni−Zn-MCM-41 is likely due to the larger mesopores that are not as susceptible to blockage from carbon deposits as the micropores in Ni-CIT-6. Selectivities to non-C_{3n} products (Figure 2) for Ni-CIT-6 are no more than 6% at any time at 180 °C. For Ni−Zn-MCM-41, propylene conversion remained stable at 6−8% throughout the reaction test; however, the selectivity to C_9 products is approximately half that observed for Ni-CIT-6. Total selectivities to non-C_{3n} products are <1% for all time-on-stream points.

The observed increase in propylene conversion and on-stream stability with the increase in pore size for the zincosilicates (from microporous Ni-CIT-6 to mesoporous Ni−Zn-MCM-41) is also consistent with that reported by Mlinar et al. in the comparison of microporous aluminosilicate Ni−Na-X to mesoporous aluminosilicate Ni−Al-MCM-41,[13] Further, hexene product isomer distributions reported for Ni−Na-X are similar to those of Ni-CIT-6, although the zincosilicate tends to produce more linear products.[8]

The Ni^{2+}-exchanged USY material initially gives the highest propylene conversion and has the lowest C_{3n} product selectivities (less than 65% at 180 °C) of any material tested. This is likely due to the presence of residual Brønsted acid sites within the FAU framework that catalyze oligomerization and cracking reactions, in addition to oligomerization at the nickel cation sites. In agreement with previous studies, high cracking activity is initially present at these strong acid sites until they deactivate, after which oligomerization proceeds more selectively.[14,27]

Figure 3 shows similar behavior for each of the four materials at 250 °C. TOS behavior for each material at 250 °C is similar to that observed at 180 °C, with a few exceptions. Propylene conversion increases with the increase in temperature for each material, with the exception of Ni-HiAl-BEA. Ni-CIT-6 gives higher selectivity to C_9 products at 250 °C than at 180 °C (∼22% versus ∼18%), with the corresponding selectivities to C_6 products decreasing (non-C_{3n} selectivities are typically less than 20%). However, more hexene products resulting from double-bond isomerization (such as 2-methyl-2-pentene) are observed at 250 °C rather than at 180 °C. A similar increase in formation of double-bond isomerization products at 250 °C relative to 180 °C is also observed for Ni−Zn-MCM-41. A slight decline in propylene conversion is observed over the reaction time profile, but the material still exhibits very stable conversion with increasing time on-stream. Total selectivities to non-C_{3n} products are again quite low (<1%) for all data points.

For Ni-HiAl-BEA, propylene conversion decreases with the increase in reaction temperature from 180 to 250 °C. This suggests that catalyst deactivation may be more rapid at the higher reaction temperature. Additionally, although carbon balances remain near 100% for both reaction tests, regeneration does not fully recover the initial catalyst activity.

At 250 °C, Ni-USY exhibits slightly reduced selectivities to C_9 products (∼30%) relative to those at 180 °C (∼30−35%), wheras total selectivities to C_6 products increase from ∼30−35% at 180 °C to 40−45% at 250 °C for most data points. Additionally, selectivities to C_4 and C_5 products have slightly decreased, and selectivities to C_7 and C_8 products have increased, suggesting increased cracking of C_9 products and reduced cracking of C_6 products at 250 °C. This could be attributed to faster deactivation of strong Brønsted acid sites at 250 °C. Although C_{3n} products were still the predominant products observed, the wide variety of cracking products and relatively low selectivity to the desired products make Ni-USY unsuitable as a selective oligomerization catalyst under these conditions.

Interestingly, selectivity for the major product, 2-methyl-2-pentene, decreases slightly with increasing TOS for the zincosilicates, but it increases with TOS for the aluminosilicates. This observation suggests that the residual acid sites in zincosilicates are not strong enough to catalyze cracking reactions but are still capable of isomerizing the primary oligomerization products. It is possible that the residual acid sites in the aluminosilicates are strong enough to catalyze cracking reactions, producing chiefly cracking products initially and leading to a relative lack of isomerization products. As these strong acid sites in the aluminosilicates deactivate with increasing TOS, the isomerization products could then begin to accumulate. These observations suggest that zincosilicates should be used if selectivity to simple oligomerization products is desired.

Further analysis of the hexene isomers formed from the oligomerization reaction also reveals that the zincosilicates typically exhibit much higher linear-to-branched ratios than the aluminosilicates. These higher linear-to-branched ratios observed for the zincosilicates are believed to be the result of a difference in the fine structural details around the nickel cation relative to that of the aluminosilicates. Figure 4 shows the linear-to-branched ratios for each material at 180 and 250 °C.

The ratios are fairly constant with TOS, with the exception of Ni-CIT-6, which exhibits a maximum before declining to a stable ratio at increasing TOS for both reaction temperatures. Ni−Zn-MCM-41 has stable linear-to-branched ratios very near 1.0 for both reaction temperatures. At 180 °C, both aluminosilicate catalysts have constant ratios of approximately 0.3, with the exception of the initial Ni-USY ratio. However, at 250 °C, Ni-HiAl-BEA has a significantly higher linear-to-

dx.doi.org/10.1021/cs501313z | ACS Catal. 2014, 4, 4189−4195

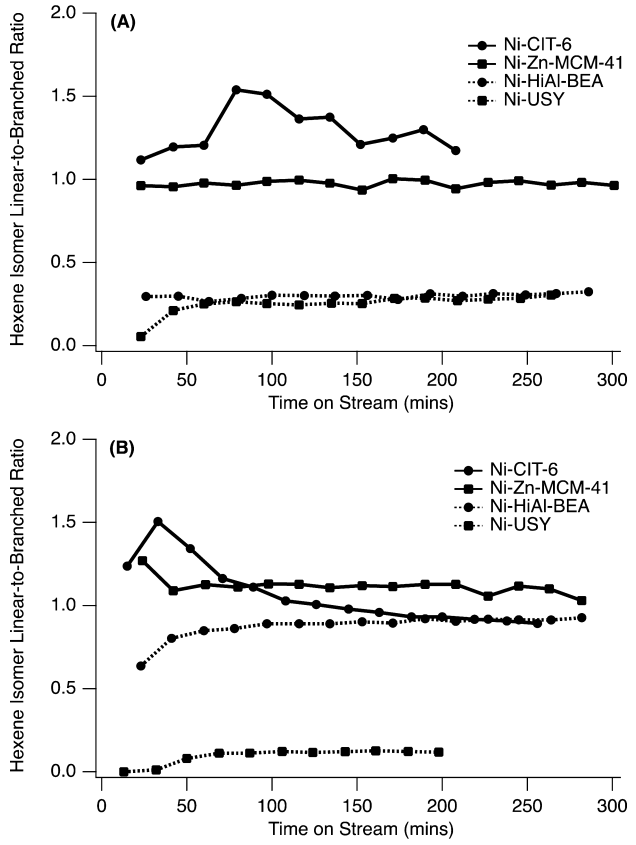

Figure 4. Hexene isomer linear-to-branched ratios for Ni-CIT-6, Ni–Zn-MCM-41, Ni-HiAl-BEA, and Ni-USY at 180 °C (A) and 250 °C (B).

branched ratio, again showing behavior similar to that of the zincosilicates at this elevated reaction temperature. The linear-to-branched ratio observed for Ni-USY at 250 °C decreases to values just above 0.1 for the duration of the reaction test. Linear hexene isomers may be useful or desirable in the synthesis of specialty chemicals, although in the synthesis of gasoline, this linearity is undesirable.

SUMMARY

Ni^{2+} ion was exchanged onto four molecular sieves, and their ability to catalyze propylene oligomerization was compared. Each material tested was capable of oligomerizing propylene, albeit with varying conversions and C_{3n} product selectivities, under the reaction conditions tested. For all catalysts except Ni-HiAl-BEA, the propylene conversion increased with increasing temperature. The opposite trend for Ni-HiAl-BEA could be due to a faster oligomerization site deactivation as temperature increases.

Double-bond isomerization from the hexenes formed directly by propylene dimerization was observed for all catalysts. Further, cracking reactions of these C_{3n} products were observed in the aluminosilicates, particularly Ni-USY (this catalyst was the least selective to C_{3n} products tested). Detailed characterization of the hexene isomers formed by each catalyst revealed that the zincosilicates also typically had much higher linear-to-branched hexene isomer ratios than the aluminosilicates. The two *BEA framework materials with zinc and aluminum heteroatoms (Ni-HiAl-BEA and Ni-CIT-6, respectively) exhibit similar time-on-stream behavior with respect to propylene conversion; however, the product distribution for Ni-HiAl-BEA is not as selective to oligomers as Ni-CIT-6, as evidenced by the relative selectivities to C_{3n} products for the two materials. Cracking products (non-C_{3n}) were also observed with Ni-HiAl-BEA. These additional cracking reactions to produce C_7 and C_8 products were likely catalyzed by the strong Brønsted acidity of the solid. Hexene selectivity and overall propylene conversion were higher at both reaction temperatures for the mesoporous Ni–Zn-MCM-41 relative to the microporous Ni-CIT-6. This was likely due to the larger pores within Ni–Zn-MCM-41, which remained unblocked by hydrocarbons for longer periods on-stream. Ni–Zn-MCM-41 had the highest, most stable conversions and highest selectivities to hexene products. Ni-USY, although it had the highest propylene conversions at each temperature, also exhibited the poorest selectivities to C_{3n} products. The wide variety of these products makes this material unsuitable as an oligomerization catalyst under the reaction conditions tested.

These observations validate the hypothesis that matching the charge of the framework heteroatom with that of the exchanged ion can reduce undesirable side reactions catalyzed by unexchanged, strong Brønsted acid sites and suggest that zincosilicates may well be interesting materials for light olefin oligomerization.

ASSOCIATED CONTENT

Supporting Information

Further characterization of the synthesized materials, as well as full reaction conversion and selectivity data are given in additional figures and tables. This material is available free of charge via the Internet at http://pubs.acs.org.

AUTHOR INFORMATION

Corresponding Author

* E-mail: mdavis@cheme.caltech.edu.

Notes

The authors declare no competing financial interest.

ACKNOWLEDGMENTS

The authors thank BP for financial support of this work through the XC^2 program.

REFERENCES

(1) O'Connor, C. T.; Kojima, M. *Catal. Today* **1990**, *6*, 329–349.
(2) Maxwell, I. E. In *Advances in Catalysis*; Eley, D. D., Pines, H., Weisz, P. B., Eds; Academic Press: New York, 1982; Vol. *31*, pp 24–38.
(3) Heveling, J.; van der Beek, A.; de Pender, M. *Appl. Catal.* **1988**, *42*, 325–336.
(4) Ng, F. T. T.; Creaser, D. C. *Appl. Catal., A* **1994**, *119*, 327–339.
(5) Bonneviot, L.; Olivier, D.; Che, M. *J. Mol. Catal.* **2001**, *21*, 415–430.
(6) Mlinar, A. N.; Baur, B. G.; Bong, G. G.; Getsoian, A.; Bell, A. T. *J. Catal.* **2012**, *296*, 156–164.
(7) Garwood, W. E.; Krambeck, F. J.; Kushnerick, J. D. Multistage Conversion of Lower Olefins with Interreactor Quenching. U.S. Patent 4,740,645, April 26, 1988.
(8) Mlinar, A. N.; Ho, O. C.; Bong, G. G.; Bell, A. T. *ChemCatChem* **2013**, *5*, 3139–3147.
(9) Hogan, J. P.; Banks, R. L.; Lanning, W. C.; Clark, A. *Ind. Eng. Chem.* **1955**, *47*, 752–757.
(10) Matsuda, T.; Miura, H.; Sugiyama, K.; Ohno, N. *J. Chem. Soc.* **1979**, 1513–1520.
(11) Kiessling, D.; Froment, G. F. *Appl. Catal.* **1991**, *71*, 123–138.

(12) Hartmann, M.; Pöppl, A.; Kevan, L. *J. Phys. Chem.* **1996**, *100*, 9906−9910.
(13) Mlinar, A. N.; Shylesh, S.; Ho, O. C.; Bell, A. T. *ACS Catal.* **2014**, *4*, 337−343.
(14) Hulea, V.; Fajula, F. *J. Catal.* **2004**, *225*, 213−222.
(15) Dědeček, J.; Sobalík, Z.; Wichterlová, B. *Catal. Rev.* **2012**, *54*, 135−223.
(16) Tanaka, M.; Itadani, A.; Kuroda, Y.; Iwamoto, M. *J. Phys. Chem. C* **2012**, *116*, 5664−5672.
(17) Serrano, D. P.; van Grieken, R.; Melero, J. A.; García, A. *Appl. Catal., A* **2004**, *269*, 137−146.
(18) Takewaki, T.; Beck, L. W.; Davis, M. E. *Top. Catal.* **1999**, *9*, 35−42.
(19) Takewaki, T.; Beck, L. W.; Davis, M. E. *J. Phys. Chem. B* **1999**, *103*, 2674−2679.
(20) Takewaki, T.; Davis, M. E. Molecular Sieve CIT-6. U.S. Patent 6,117,411, September 12, 2000.
(21) Majano, G.; Delmotte, L.; Valtchev, V.; Mintova, S. *Chem. Mater.* **2009**, *21*, 4184−4191.
(22) Kamimura, Y.; Chaikittisilp, W.; Itabashi, K.; Shimojima, A.; Okubo, T. *Chem.—Asian J.* **2010**, *5*, 2182−2191.
(23) Chaikittisilp, W.; Yokoi, T.; Okubo, T. *Microporous Mesoporous Mater.* **2008**, *116*, 188−195.
(24) Takewaki, T.; Hwang, S.-J.; Yamashita, H.; Davis, M. E. *Microporous Mesoporous Mater.* **1999**, *32*, 265−278.
(25) Hartmann, M.; Racouchot, S.; Bischof, C. *Chem. Commun.* **1997**, 2367−2368.
(26) Hartmann, M.; Racouchot, S.; Bischof, C. *Microporous Mesoporous Mater.* **1999**, *27*, 309−320.
(27) Ghosh, A. K.; Kydd, R. A. *J. Catal.* **1986**, *100*, 185−195.